Synthesis and Characterization of $(\eta^5\text{-}C_5Me_5)_2Mo_2Fe_2(CO)_9(\mu_2\text{-}CO)(\eta^2,\mu_4\text{-}CO)$, a 62-Electron Butterfly Molybdenum–Iron Cluster Containing a π-Bound Four-Electron-Donating Carbonyl Ligand: A Possible Structural Model for the Active Dinitrogen Molybdenum–Iron Site in Nitrogenase

Charles P. Gibson[1] and Lawrence F. Dahl*

Department of Chemistry, University of Wisconsin—Madison, Madison, Wisconsin 53706

Received October 14, 1986

The photolytic reaction of a toluene suspension of $Fe_2(CO)_9$ and $Mo_2(\eta^5\text{-}C_5Me_5)_2(CO)_4$ under O_2-free conditions gave as the major product (12–24% yields) a new butterfly Mo–Fe cluster, $(\eta^5\text{-}C_5Me_5)_2Mo_2Fe_2(CO)_9(\mu_2\text{-}CO)(\eta^2,\mu_4\text{-}CO)$ (1), which was characterized from spectroscopic (IR and ^1H and ^{13}C NMR), electrochemical, and X-ray diffraction measurements. The solid-state configuration of 1 consists of an edge-opened tetrahedral (butterfly) metal fragment with two iron atoms in the hinge positions and two molybdenum atoms in the wingtip positions. A π-bound carbonyl ligand is coordinated to all four metal atoms via a capping linkage of the carbon atom with a $MoFe_2$ triangle and a η^2 attachment of the carbon and oxygen atoms by a presumed π-donating orbital to the other wingtip molybdenum atom. The formation of 1 can be envisioned to occur by the cycloaddition of two photolytically generated $Fe(CO)_4$ fragments across the formal Mo–Mo triple bond of $Mo_2(\eta^5\text{-}C_5Me_5)_2(CO)_4$ to give a bicyclobutane-like 62-electron product that could convert into the 62-electron 1 by the following sequence: (1) the photoinduced loss of one carbonyl ligand; (2) a concerted Mo–Mo bond-breaking and Fe–Fe bond-making process; and (3) a carbonyl-ligand rearrangement featuring the insertion of a carbonyl group into the resulting butterfly Mo_2Fe_2 cavity and the formation of a hinge-bridging carbonyl group across the Fe–Fe bond. The highly unusual butterfly-bridging carbonyl ligand, which is presumed to function as a four-electron donor, has previously been reported only for the prototype $[Fe_4(CO)_{12}(\mu_2\text{-}H)(\eta^2,\mu_4\text{-}CO)]^-$ monoanion (2) and closely related $[Fe_4(CO)_{12}(\mu_2\text{-}X)(\eta^2,\mu_4\text{-}CO)]^-$ monoanions containing other Lewis acid, hinge-bridging $(\mu_2\text{-}X)^+$ ligands (e.g., X = $AuPEt_3$ (3); X = $CuPPh_3$; X = HgMe). The π-bound carbonyl ligand in 1 gives rise to a characteristic low-frequency carbonyl IR band at 1320 cm^{-1} and a low-field ^{13}C NMR resonance at δ 274; these spectroscopic features are similar to those found in the above-mentioned butterfly isomers of the tetrairon monoanions. A cyclic voltammogram of 1 in CH_2Cl_2 exhibited a quasi-reversible oxidation couple at an $E_{1/2}$ value of +0.568 V vs SCE (ΔE_p = 81 mV). On the basis of the geometrical features of 1, a structural model is presented for the *active site* of nitrogenase. This enzyme contains two structurally unknown molybdenum–iron prosthetic cores (each composed of one Mo and six to eight Fe atoms) that fix (convert) dinitrogen molecules to ammonia. The proposed structural model involves a butterfly-like $MoFe_3$ fragment containing a π-bound N_2 molecule. The subsequent protonation–reduction transformations needed to produce two NH_3 molecules from the η^2-coordinated N_2 ligand are presumed to include a proton-induced reductive N–N bond cleavage to give one NH_3 molecule and an intermediate butterfly-like $MoFe_3(\mu_4\text{-}N)$ fragment of an iron–molybdenum core.

Introduction

Several rational synthetic strategies have recently been shown to be effective for the production of new organometallic clusters in relatively high yields.[2-5] One notable example involves the synthesis of 48-electron triangular metal clusters via the addition of reactive, coordinatively unsaturated 16-electron organometallic fragments across the formal metal–metal double bond of various 32-electron organometallic dimers.[4,5] Hoffmann[6] and Stone[7] have pointed out that such reactions may be considered as inorganic equivalents of the reaction of methylene and ethylene to form cyclopropane since 16-electron organometallic species such as $Fe(CO)_4$ and $Co(\eta^5\text{-}C_5Me_5)(CO)$ and 32-electron organometallic dimers such as $Co_2(\eta^5\text{-}C_5Me_5)_2(\mu_2\text{-}CO)_2$ are isolobal with methylene and ethylene, respectively.

As an extension of our work[5] in this area, we have attempted to add photolytically generated, coordinatively unsaturated organometallic moieties across the formal Mo–Mo triple bond of the 30-electron $Mo_2(\eta^5\text{-}C_5Me_5)_2$-

(1) This work was taken in part from the Ph.D. thesis of C. P. Gibson. University of Wisconsin—Madison, 1985. Present Address: Department of Chemistry, West Virginia University, Morgantown, WV 26506.

(2) Gladfelter, W. L.; Geoffroy, G. L. *Adv. Organomet. Chem.* **1980**, *18*, 207–273 and references cited therein.

(3) Roberts, D. A.; Geoffroy, G. L. In *Comprehensive Organometallic* Chemistry; Wilkinson, G., Ed.; Pergamon: New York, 1982; Vol. 6, and references cited therein.

(4) (a) Ashworth, T. V.; Howard, J. K.; Stone, F. G. A. *J. Chem. Soc., Chem. Commun.* **1979**, 42–43. (b) Green, M.; Mills, R. M.; Pain, G. N.; Stone, F. G. A.; Woodward, P. *J. Chem. Soc., Dalton Trans.* **1982**, 1309–1319. (c) Boag, N. M.; Green, M.; Mills, R. M.; Pain, G. N.; Stone, F. G. A.; Woodward, P. *J. Chem. Soc., Chem. Commun.* **1980**, 1171–1173. (d) Farrugia, L. J.; Howard, J. A. K.; Mitrprachachon, P.; Stone, F. G. A.; Woodward, P. *J. Chem. Soc., Dalton Trans.* **1981**, 155–161. (d) Farrugia, L. J.; Howard, J. A. K.; Mitrprachachon, P.; Stone, F. G. A.; Woodward, P. *J. Chem. Soc., Dalton Trans.* **1981**, 171–179. (f) Brun, P.; Dawkins, G. M.; Green, M.; Miles, A. D.; Orpen, A. G.; Stone, F. G. A. *J. Chem. Soc., Chem. Commun.* **1982**, 926–927. (g) Barr, R. D.; Green, M.; Howard, J. A. K.; Marder, T. B.; Stone, F. G. A. *J. Chem. Soc., Chem. Commun.* **1983**, 759–760. (h) Green, M.; Hankey, D. R.; Howard, J. A. K.; Louca, P.; Stone, F. G. A. *J. Chem. Soc., Chem. Commun.* **1983**, 757–758.

(5) (a) Cirjak, L. M.; Huang, J.-S.; Zhu, Z.-H.; Dahl, L. F. *J. Am. Chem. Soc.* **1980**, *102*, 6623–6626. (b) Cirjak, L. M. Ph.D. Thesis, University of Wisconsin—Madison, 1980. (c) Olson, W. L.; Stacy, A. M.; Dahl, L. F. *J. Am. Chem. Soc.* **1986**, *108*, 7646–7656.

(6) Hoffmann, R. *Angew. Chem., Int. Ed. Engl.* **1982**, *21*, 711–724 and references cited therein.

(7) Stone, F. G. A. *Angew. Chem., Int. Ed. Engl.* **1984**, *23*, 89–99.

0276-7333/88/2307-0535$01.50/0

$(CO)_4$ (4),[8] an isolobal analogue of acetylene. The anticipated products of the specific reaction of $Fe(CO)_4$ fragments with 4 are illustrated in Scheme I. In this example, a coordinatively unsaturated 16-electron $Fe(CO)_4$ fragment (photolytically generated from $Fe_2(CO)_9$) could add across the formal Mo–Mo triple bond of 4 to give the new cyclopropene-like, 46-electron dimolybdenum–iron cluster 5. Further reaction of 5 with a second 16-electron $Fe(CO)_4$ moiety might be expected to give the new bicyclobutane-like, 62-electron dimolybdenum–diiron cluster 6.

An initial attempt to add photolytically generated $Fe(CO)_4$ fragments to 4 by photolysis of a toluene suspension of $Fe_2(CO)_9$ and 4 under a slow N_2 stream led instead to the isolation and stereochemical characterization of a new 48-electron oxo-capped dimolybdenum–iron cluster, $(\eta^5\text{-}C_5Me_5)_2Mo_2Fe(CO)_7(\mu_3\text{-}O)$, as the only mixed-metal product.[9,10] We then discovered that the oxo-capped atom was derived from O_2 which was inadvertently added to the reaction vessel; pretreatment of a toluene suspension of $Fe_2(CO)_9$ and 4 with either pure O_2 or air prior to the photolysis gave $(\eta^5\text{-}C_5Me_5)_2Mo_2Fe(CO)_7(\mu_3\text{-}O)$ in nonoptimized yields of 16–24%.[10]

Herein we report that when the reaction is run under O_2-free conditions, a dimolybdenum–diiron cluster, $(\eta^5\text{-}C_5Me_5)Mo_2Fe_2(CO)_9(\mu_2\text{-}CO)(\eta^2,\mu_4\text{-}CO)$ (1), is the only new mixed-metal species recovered.[9] A structural determination of 1 revealed it to contain an open-edge tetrahedral (butterfly) fragment of metal atoms coordinated to a π-bound carbonyl ligand. This rare butterfly-bridging carbonyl ligand has been previously found only in the $[Fe_4(CO)_{12}(\mu_2\text{-}X)(\eta^2,\mu_4\text{-}CO)]^-$ monoanions (X = H (2);[11] X = $AuPEt_3$ (3), $AuPPh_3$; X = $CuPPh_3$, $Cu(CNC_6H_3Me_2\text{-}2,6)$; X = HgMe) formed by the addition of a proton[11] or other X^+ Lewis acid[12–14] to the 60-electron $[Fe_4(CO)_{12}(\mu_3\text{-}CO)]^{2-}$ dianion.[15] In 1979 Muetterties and Stein[16] suggested that this η^2 linkage of both the carbonyl carbon and oxygen atoms in the prototype $[Fe_4(CO)_{12}(\mu_2\text{-}H)(\eta^2,\mu_4\text{-}CO)]^-$ monoanion (2) may be a molecular analogue of an intermediate state in the cleavage of chemisorbed carbon monoxide on a metal surface, such as occurs in Fischer–Tropsch catalysis.[16,17] This monoanion (2) was also implicated by Shriver and co-workers[18–20] as a polynuclear metal intermediate in the proton-induced reduction of the μ_3-coordinated carbon monoxide in the $[Fe_4(CO)_{12}(\mu_3\text{-}CO)]^{2-}$ dianion into methane.[18–20]

This paper describes the details of the synthesis, the molecular structure and bonding, and the physical–chemical properties of the dimolybdenum–diiron cluster (1). Since both infrared and ^{13}C spectral data provide definite evidence that the C–O bond strength of the π-bound carbonyl ligand in 1 is analogous to those in 2 and 3 and thus substantially less than that of either a free or terminal carbonyl group, this particular ligation of both the carbon and oxygen atoms presents a plausible model for similar multimetal interactions promoting bond cleavage of other cordinated molecules such as N_2. In fact, the mode of attachment of this four-electron-donating carbonyl ligand in 1 has formed the basis for our proposal (presented herein) of a structural model for the active site for the fixation of the isoelectronic dinitrogen molecule in nitrogenase.

Experimental Section

General Procedures. All manipulations were carried out under an atmosphere of prepurified nitrogen either with standard Schlenk and high-vacuum techniques or within a Vacuum Atmospheres glovebox. The following solvents were freshly distilled from the indicated drying agent and saturated with N_2 immediately prior to use: hexane (CaH_2), dichloromethane (P_2O_5), and toluene (sodium/benzophenone). Benzene-d_6, chloroform-d_1, and dichloromethane-d_2 were dried over molecular sieves and vacuum-distilled prior to use. Triflic acid and methyl triflate were vacuum-distilled prior to use. $Mo_2(\eta^5\text{-}C_5Me_5)_2(CO)_4$ and $Fe_2(CO)_9$ were prepared via slight modifications of published procedures.[21,22] Since natural abundance ^{13}C NMR spectra of 1 indicate that the carbonyl ligands are completely scrambled at room temperature (vide infra), samples of 1 enriched to 12% ^{13}CO were prepared from ^{13}CO-enriched $Mo_2(\eta^5\text{-}C_5Me_5)_2(CO)_4$. All other reagents were purchased from major chemical suppliers and used without further purification.

Infrared spectra were recorded on a Beckman Model 4240 spectrophotometer either in the solid state as a KBr disk or in solution with 0.1-mm path-length KBr solution cells. Proton NMR spectra were recorded on either a Bruker WP-200 or a Bruker WP-270 spectrometer and were referenced indirectly to TMS by use of residual solvent protons. ^{13}C NMR spectra were recorded at 213 K on a JEOL FX-200 spectrometer operated at 50.45 MHz and were referenced indirectly to TMS via the solvent resonance. Cyclic voltammetric measurements were performed in dichloromethane as previously described[23] with a Bioanalytical Systems electrochemical analyzer, Model 100, equipped with a PAR electrochemical cell which was operated within a Vacuum Atmospheres glovebox.

Chromatographic separations were performed with Ace Glass medium-pressure chromatographic accessories that were modified to handle air-sensitive materials. The columns were packed with 80–200 mesh Brockman activity I neutral alumina and were prepared in hexane.

Preparation of $(\eta^5\text{-}C_5Me_5)_2Mo_2Fe_2(CO)_9(\mu_2\text{-}CO)(\eta^2,\mu_4\text{-}CO)\cdot C_7H_8$ (1·tol). In a typical reaction, a mixed sample of

(8) Huang, J.-S.; Dahl, L. F. *J. Organomet. Chem.* **1983**, *243*, 57–68.

(9) Gibson, C. P.; Mahood, J. A.; Huang, J.-S.; Dahl, L. F. *Abstracts of Papers*, 187th National Meeting of American Chemical Society St. Louis, MO; American Chemical Society: Washington, DC, 1984; INOR 202.

(10) Gibson, C. P.; Huang, J.-S.; Dahl, L. F. *Organometallics* **1986**, *5*, 1676–1681.

(11) (a) Manassero, M.; Sansoni, M.; Longoni, G. *J. Chem. Soc., Chem. Commun.* **1976**, 919–920. (b) Hieber, W.; Werner, R. *Chem. Ber.* **1957**, *90*, 286–296.

(12) Horwitz, C. P.; Shriver, D. F. *Organometallics* **1984**, *3*, 756–758.

(13) (a) Horwitz, C. P.; Holt, E. M.; Shriver, D. F. *J. Am. Chem. Soc.* **1985**, *107*, 281–282. (b) Horwitz, C. P.; Holt, E. M.; Brock, C. P.; Shriver, D. F. *J. Am. Chem. Soc.* **1985**, *107*, 8136–8146.

(14) Horwitz, C. P.; Shriver, D. F. *J. Am. Chem. Soc.* **1985**, *107*, 8147–8153.

(15) (a) Doedens, R. J.; Dahl, L. F. *J. Am. Chem. Soc.* **1986**, *88*, 4847–4855. (b) Buskirk, G. van; Knobler, C. B.; Kaesz, H. D. *Organometallics* **1985**, *4*, 149–153.

(16) Muetterties, E. L.; Stein, J. *Chem. Rev.* **1979**, *79*, 479–490.

(17) (a) Sachtler, W. M. H.; Shriver, D. F.; Hollenberg, W. B.; Lang, A. F. *J. Catal.* **1985**, *92*, 429–431. (b) Herrmann, W. A. *Angew. Chem., Int. Ed. Engl.* **1982**, *21*, 117–130, and references cited therein. (c) Biloen, P.; Sachtler, W. M. H. *Adv. Catal.* **1981**, *30*, 165–216. (d) Masters, C. *Adv. Organomet. Chem.* **1979**, *17*, 61–103 and references cited therein.

(18) Whitmire, K. H.; Shriver, D. F. *J. Am. Chem. Soc.* **1980**, *102*, 1456–1457.

(19) (a) Whitmire, K. H.; Shriver, D. F.; Holt, E. M. *J. Chem. Soc., Chem. Commun.* **1980**, 780–781. (b) Holt, E. M.; Whitmire, K. H.; Shriver, D. F. *J. Organomet. Chem.* **1981**, *213*, 125–137. (c) Whitmire, K. H.; Shriver, D. F. *J. Am. Chem. Soc.* **1981**, *103*, 6754–6755. (d) Drezdzon, M. A.; Whitmire, K. H.; Bhattacharyya, A. A.; Hsu, W.-L.; Nagel, C. C.; Shore, S. G.; Shriver, D. F. *J. Am. Chem. Soc.* **1982**, *104*, 5630–5633. (e) Drezdzon, M. A.; Shriver, D. F. *J. Mol. Catal.* **1983**, *21*, 81–93.

(20) Horwitz, C. P.; Shriver, D. F. *Adv. Organomet. Chem.* **1984**, *23*, 219–303 and references cited therein.

(21) King, R. B.; Iqbal, M. Z.; King, A. D., Jr. *J. Organomet. Chem.* **1979**, *171*, 53–63.

(22) King, R. B. *Organometallic Synthesis*; Academic: New York, 1965; Vol. 1, pp 93–95.

(23) Bedard, R. L.; Dahl, L. F. *J. Am. Chem. Soc.* **1986**, *108*, 5933–5942.

$Fe_2(CO)_9$ (1.00 g, 2.74 mmol) and $Mo_2(\eta^5\text{-}C_5Me_5)_2(CO)_4$ (**3**) (1.00 g, 1.74 mmol) was placed in a water-cooled quartz immersion-well photolysis unit which was equipped with a large magnetic stir bar. Toluene was added, and the stirred suspension was irradiated for approximately 4 h with a Hanovia 450-W, medium-pressure Hg vapor lamp. A slow stream of N_2 was bubbled through the solution during the photolysis reaction in order to assist in the mixing of the solution as well as to facilitate the removal of liberated carbon monoxide.

The contents of the reaction vessel were transferred to a flask, and the solvent was evaporated. Small quantities of alumina and dichloromethane were added to the remaining brown tar. The resulting brown suspension was mixed thoroughly, and the solvent was then evaporated to give a brown powder that was carefully loaded onto the top of a chromatographic column containing alumina. Elution with a solution of hexane–toluene (50/50 v/v) resulted in the isolation of a red-orange band containing **3** and $Mo_2(\eta^5\text{-}C_5Me_5)_2(CO)_6$ that were identified by their characteristic infrared and ^1H NMR spectra. Subsequent elution with toluene alone produced a rather broad, brown band that contained primarily **1**. Evaporation of the solvent from this band in a stream of N_2 afforded a large number of black needles on top of a small amount of brown powder. The black crystals were carefully separated from the brown powder. Recrystallization of the crystals from toluene gave ca. 200–400 mg (0.21–0.42 mmol, 12–24% yield) of **1**·tol as black needles. An infrared spectrum of **1** in benzene (Figure 1, supplementary material) displayed absorbances at 2025 (w), 1900 (vs), 1980 (vs), 1936 (m), 1896 (sh), 1829 (w), 1380 (w), and 1340 (w) cm^{-1}. A ^1H NMR spectrum of **1** in C_6D_6 exhibited resonances at δ 1.59 (s, 15 H) and 1.69 (s, 15 H) due to the pentamethylcyclopentadienyl ligands. A ^1H NMR spectrum of **1** in CD_2Cl_2 displayed resonances at δ 1.95 (s, 15 H) and 1.99 (s, 15 H). Low-temperature ^{13}C spectra in CD_2Cl_2 (Figure 2, supplementary material) displayed resonances at δ 274.0, 241.4, 232.4, 226.1, and 216.3 with relative intensities 1:1:1:2:6; these peaks were assigned to the various carbonyl carbon atoms of **1** (vide infra). Cyclic voltammetric measurements revealed that **1** in CH_2Cl_2 solution undergoes a quasi-reversible oxidation at +0.568 V vs SCE (Figure 3, supplementary material). Attempts to isolate an oxidized form of **1** from the products of the reaction of **1** with $AgPF_6$ were unsuccessful. No reaction occurred between **1** and a slight excess of triflic acid in CH_2Cl_2 at 20 °C. There was also no reaction between **1** and methyl triflate under similar conditions.

Crystallographic Determination of the Structure of $(\eta^5\text{-}C_5Me_5)_2Mo_2Fe_2(CO)_9(\mu_2\text{-}CO)(\eta^2,\mu_4\text{-}CO)\cdot C_7H_8$ (1·tol). Well-formed black needle crystals of **1**·tol were grown by the slow evaporation of a toluene solution of **1**. Preliminary optical and X-ray examination of several crystals and collection of intensity data were carried out on a Syntex (Nicolet) P$\bar{1}$ diffractometer with graphite-monochromated Mo K$\bar{\alpha}$ radiation. Axial photographs were utilized to verify the approximate dimensions and symmetry of the chosen orthorhombic unit cell. Refined lattice constants were determined from a least-squares analysis of setting angles for 15 centered, high-angle reflections. The procedures involved in the crystal alignment and data collection are described elsewhere.[24] The intensities of three standard reflections, which were periodically monitored throughout each data collection, did not show significant variations (<4%).

Systematic absences of $0kl$ for $k + l$ odd and $h0l$ for h odd indicated that the probable space groups were $Pna2_1$ (C_{2v}^9, No. 33) and $Pnam$ (D_{2h}^{16}, No. 62, a nonstandard setting of $Pnma$).[25] Our initial selection of the acentric group, $Pna2_1$, was based on the close correlation of the Wilson plot of the normalized structure factors with a noncentrosymmetric distribution. Only for the acentric group was a meaningful solution of the structure obtained by direct methods[26] and by an interpretation of a Patterson map. The solution that was obtained and subsequently refined in the space group $Pna2_1$ could not be forced into the centrosymmetric space group $Pnam$ (with molecular C_s—m site symmetry).

Table I. Crystal Data and Details of Data Collection and Refinement of $(\eta^5\text{-}C_5Me_5)_2Mo_2Fe_2(CO)_9(\mu_2\text{-}CO)(\eta^2,\mu_4\text{-}CO)\bullet C_7H_8$

fw	974.3
cryst system	orthorhombic
cell constants (23 °C)	
a, b, c (Å)	30.628 (13), 14.074 (6), 8.944 (3)
V (Å^3)	3858
space group	$Pna2_1$
Z	4
d_{calcd} (g/cm^3)	1.68
radiatn (λ, Å)	Mo K$\bar{\alpha}$ (0.71073)
data collection temp, °C	23 °C
scan mode	ω
2θ limits (deg)	4–50
scan speed (deg/min)	variable (1.0–29.3)
scan width (deg above $K\alpha_1$/below $K\alpha_2$)	0.8/0.8
std rfltns/frequency	363; 451; 10,1,0/3 per 47
cutoff obsd data	$I > 3.0\sigma(I)$
no. of indep obsd. data	2134
no. of parameters	173
data-to-parameter ratio	12.3/1
$R_1(F)$, $R_2(F)$ (%)	8.41, 11.22

Because of a crystal-disordered problem (vide infra) encountered during the latter stages of the refinement of the structure of **1**·tol, we obtained three different sets of intensity data from different crystals of **1**·tol. Both empirical and analytical absorption corrections[27-30] were applied to all of the data sets. No substantial differences in the final structural parameters were obtained for the various sets of data. The crystallographic results that are quoted throughout the text and presented in Tables I–III were based on a data set (Table I) treated in the following manner.

A needle-shaped crystal of dimensions 0.4 × 0.1 × 0.1 mm was glued with epoxy resin inside an argon-filled Lindemann glass capillary that was then hermetically sealed. Initial positions of the metal atoms were determined by direct methods[26] and confirmed from a Patterson map. The remaining non-hydrogen atoms were located from a combination of successive difference maps coupled with several cycles of isotropic least-squares refinement with RAELS.[29] At this point, the pentamethylcyclopentadienyl ligands were introduced into the refinement as rigid groups with local C_{5v} symmetry. Both the positional and thermal parameters for the rigid groups were refined by use of subsidiary axial systems as described by Rae.[31,32] Hydrogen atoms of these ligands were included at idealized positions but were not refined. During a later stage of refinement, the methyl substituents of each pentamethylcyclopentadienyl ligand were individually allowed to move away from the plane containing the five ring carbon atoms. A Fourier difference map indicated the presence of a disordered

(24) Byers, L. R.; Dahl, L. F. *Inorg. Chem.* **1980**, *19*, 277–284.

(25) *International Tables for X-ray Crystallography*; Kynoch: Birmingham, England, 1985; Vol. I, pp 119, 151.

(26) (a) Main, P.; Lessinger, L.; Woolfson, M. M.; Germain, G.; Declercq, J.-P. MULTAN-76. (b) Germain, G.; Main, P.; Woolfson, M. M. *Acta Crystallogr., Sect. A: Cryst. Phys., Diffr., Theor. Gen. Crystallogr.* **1971**, *A27*, 368–376.

(27) An absorption tensor is computed from ΔF values by use of an option of the program RAELS.[28,29] This correction, based on an empirical spherical haromonic model, is similar to that used by Hope.[30]

(28) Rae, A. D. *The Refinability of Absorption Corrections*", presented at the Annual Meeting of the American Crystallographic Association; McMaster University; Hamilton, Ontario, Canada; June 22–27, 1986; Abstract PA14.

(29) Rae, A. D. RAELS, A Comprehensive Least-Squares Program; University of New South Wales: Kensington, 1976; adapted for a Harris/7 computer by A. D. Rae, University of Wisconsin—Madison, 1983.

(30) Hope, H., personal communication (Feb 1984) to L. F. Dahl. The Hope program ABSORPTION (Hope, H.; Moezzi, B., unpublished results) utilizes an empirical absorption tensor from an expression relating $|F_o|$ and $|F_c|$.

(31) Rae, A. D. *Acta Crystallogr., Sect. A: Cryst. Phys., Diffr., Theor. Gen. Crystallogr.* **1975**, *A31*, 560–569.

(32) Although the hydrogen atoms were placed in idealized positions, RAELS[29] provides estimated standard deviations for these atoms. These estimates reflect the errors associated with the orientations of the local axial systems (which are calculated from the crystallographic coordinates of the ring carbon atoms) and do not reflect actual estimated standard deviations of the fractional coordinates of these atoms. Likewise, the thermal parameters and associated estimated standard deviations reported for the hydrogen atoms are not meant to imply that these parameters have been determined accurately for this structure. These values arise from the calculation of the librational-like motion of the $\eta^5\text{-}C_5Me_5$ group.

Table II. Fractional Atomic Coordinates for $(\eta^5\text{-}C_5Me_5)_2Mo_2Fe_2(CO)_9(\mu_2\text{-}CO)(\eta^2,\mu_4\text{-}CO)\cdot C_7H_8$

atom	x	y	z
Mo(1)	0.4063 (1)	0.2277 (2)	0.4789 (0)
Mo(2)	0.2782 (1)	0.1341 (2)	0.6543 (5)
Fe(1)	0.3514 (2)	0.0632 (3)	0.4858 (8)
Fe(2)	0.3637 (2)	0.1528 (3)	0.7296 (7)
C	0.3404 (15)	0.2195 (35)	0.5231 (53)
O	0.3038 (6)	0.2470 (13)	0.5173 (21)
C(1)	0.3801 (13)	0.2388 (28)	0.2818 (45)
O(1)	0.3644 (8)	0.2591 (18)	0.1730 (32)
C(2)	0.3820 (9)	0.3511 (22)	0.5186 (33)
O(2)	0.3688 (9)	0.4315 (19)	0.5466 (30)
C(3)	0.3275 (12)	−0.0418 (29)	0.5491 (45)
O(3)	0.3147 (10)	−0.1232 (26)	0.5795 (37)
C(4)	0.3167 (12)	0.0803 (27)	0.3272 (46)
O(4)	0.2949 (9)	0.0929 (20)	0.2314 (35)
C(5)	0.3910 (12)	0.0055 (26)	0.3801 (44)
O(5)	0.4145 (10)	−0.0324 (25)	0.3126 (40)
C(6)	0.2882 (11)	0.0324 (24)	0.8032 (40)
O(6)	0.2919 (10)	−0.0241 (23)	0.8971 (41)
C(7)	0.2940 (12)	0.2095 (27)	0.8337 (45)
O(7)	0.2923 (8)	0.2609 (18)	0.9263 (29)
C(8)	0.3887 (13)	0.2487 (31)	0.7880 (47)
O(8)	0.3996 (10)	0.3215 (22)	0.8617 (36)
C(9)	0.4001 (12)	0.0561 (25)	0.6547 (50)
O(9)	0.4268 (7)	−0.0007 (16)	0.6912 (24)
C(10)	0.3699 (12)	0.0886 (26)	0.8910 (45)
O(10)	0.3763 (10)	0.0539 (22)	1.0133 (39)
Cp(1)	0.4713 (9)	0.2082 (11)	0.3327 (24)
Cp(2)	0.4654 (8)	0.3053 (13)	0.3726 (21)
Cp(3)	0.4699 (7)	0.3130 (13)	0.5305 (20)
Cp(4)	0.4786 (9)	0.2207 (11)	0.5883 (23)
Cp(5)	0.4795 (7)	0.1559 (14)	0.4661 (19)
Me(1)	0.4748 (13)	0.1713 (15)	0.1804 (25)
Me(2)	0.4633 (13)	0.3853 (16)	0.2674 (25)
Me(3)	0.4758 (12)	0.4031 (16)	0.6139 (25)
Me(4)	0.4921 (14)	0.1991 (15)	0.7421 (26)
Me(5)	0.4976 (10)	0.0579 (16)	0.4718 (25)
Cp(6)	0.2133 (8)	0.2139 (14)	0.6475 (18)
Cp(7)	0.2102 (7)	0.1360 (11)	0.7497 (23)
Cp(8)	0.2116 (8)	0.0499 (14)	0.6650 (18)
Cp(9)	0.2157 (7)	0.0746 (12)	0.5105 (21)
Cp(10)	0.2167 (8)	0.1759 (12)	0.4997 (22)
Me(6)	0.2074 (14)	0.3171 (16)	0.6865 (25)
Me(7)	0.1974 (12)	0.1437 (15)	0.9133 (27)
Me(8)	0.2036 (12)	−0.0484 (16)	0.7253 (24)
Me(9)	0.2114 (14)	0.0066 (16)	0.3806 (26)
Me(10)	0.2171 (12)	0.2324 (15)	0.3576 (26)
TC(1A)	0.5975 (8)	0.4038 (17)	0.4102 (74)
TC(2A)	0.6005 (11)	0.4144 (25)	0.5651 (75)
TC(3A)	0.6003 (13)	0.3371 (38)	0.6965 (99)
TC(4A)	0.5957 (11)	0.2439 (27)	0.5949 (74)
TC(5A)	0.5928 (8)	0.2333 (17)	0.4401 (74)
TC(6A)	0.5938 (5)	0.3135 (17)	0.3507 (71)
TC(7A)	0.5905 (11)	0.3018 (29)	0.1791 (71)
TC(1B)	0.5958 (9)	0.3975 (19)	0.3184 (67)
TC(2B)	0.5987 (9)	0.4081 (19)	0.4733 (68)
TC(3B)	0.5978 (8)	0.3280 (25)	0.5627 (64)
TC(4B)	0.5940 (9)	0.2376 (20)	0.5032 (68)
TC(5B)	0.5910 (9)	0.2271 (17)	0.3483 (69)
TC(6B)	0.5920 (8)	0.3073 (22)	0.2589 (64)
TC(7B)	0.5888 (14)	0.2955 (38)	0.0873 (64)

toluene of crystallization in two orientations (Figure 4, supplementary material). Proton NMR data verified the existence of a toluene molecule of crystallization for each molecule of **1**. The geometry of the toluene molecule was modeled as a superposition of two rigid groups. Attempts to refine the occupancies (α and $1-\alpha$) of the two orientations were unsuccessful; consequently, three parallel refinements were conducted with the occupancies of the two orientations of the disordered toluene molecule fixed at values of 0.67/0.33, 0.5/0.5, and 0.33/0.67. Each of these three refinements produced similar positional and thermal parameters for the butterfly Mo_2Fe_2 molecule.[31-33] The results reported herein

(33) Rae, A. D. *Acta Crystallogr., Sect. A: Cryst. Phys., Diffr., Theor. Gen. Crystallogr.* **1975**, *A31*, 570–574.

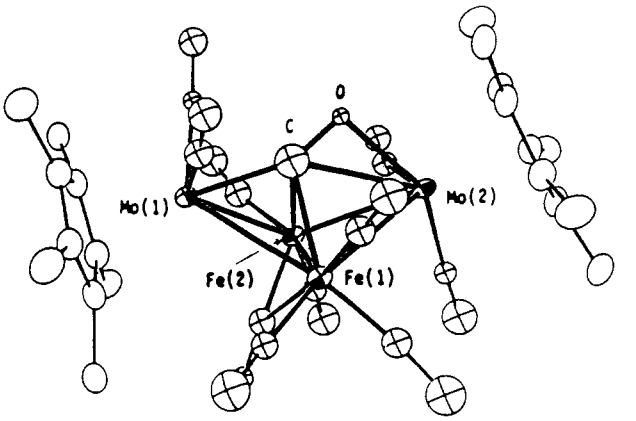

Figure 5. Molecular geometry of $(\eta^5\text{-}C_5Me_5)_2Mo_2Fe_2(CO)_9(\mu_2\text{-}CO)(\eta^2,\mu_4\text{-}CO)$ (1). This 62-electron system possesses a butterfly-like Mo_2Fe_2 core with two iron atoms in the hinge positions and two molybdenum atoms in the wingtip positions. A π-bound four-electron-donating bridging carbonyl ligand is coordinated to all four metal atoms through its carbon atom and to one of the wingtip molybdenum atoms, Mo(2), through its oxygen atom. The anomalously large thermal ellipsoid for the bridging μ_4-carbon atom is due to a crystal disorder.

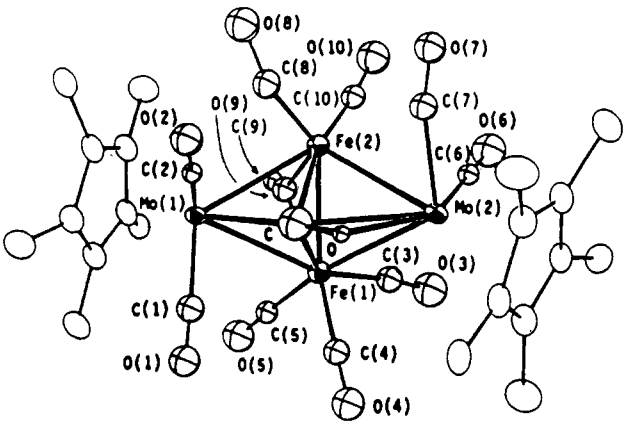

Figure 6. Another view of the molecular geometry of $(\eta^5\text{-}C_5Me_5)_2Mo_2Fe_2(CO)_9(\mu_2\text{-}CO)(\eta^2,\mu_4\text{-}CO)$ showing the highly unusual metal linkage of the carbonyl ligand within the butterfly-like Mo_2Fe_2 cavity. The anomalous difference in sizes of the isotropic atomic thermal ellipsoids for this π-bound carbonyl ligand is attributed to a crystal disorder.

are for the refinement conducted with the two alternative toluene positions equally occupied.

The final refinement was performed with anisotropic thermal parameters used for the metal atoms and isotropic thermal parameters used for the carbonyl ligands.[34,35] A TLX thermal model was used for each $(\eta^5\text{-}C_5Me_5)$ ligand, while a T model was used for the disordered toluene molecule.[31-33] Each parameter change-to-esd ratio in the final cycle was less than 0.1. A final difference map revealed several small residual electron-density peaks interspersed among the carbonyl ligands. Although a number of the carbonyl ligands appeared to be disordered, a simple model of the disorder was not found.

Effects of anomalous dispersion[35] on the structure in the noncentrosymmetric space group were taken into account by conducting a least-squares refinement in which the signs of all atomic coordinates were changed; this refinement converged at

(34) The unweighted and weighted discrepancy factors used are $R_1(F) = [\sum||F_o| - |F_c||/\sum|F_o|] \times 100$ and $R_2(F) = [\sum w_i||F_o| - |F_c||^2/\sum w_i|F_o|^2]^{1/2} \times 100$. All least-squares refinements were based on the minimization of $\sum w_i||F_o| - |F_c||^2$ with individual weights of $w_i = 1/\sigma^2(F_o)$ assigned on the basis of the estimated standard deviations of the observed structure factors. Atomic scattering factors and anomalous dispersion corrections were taken from ref 35.

(35) *International Tables for X-ray Crystallography*, Kynoch: Birmingham, England, 1974; Vol. IV, pp 149, 155–158.

Table III. Selected Interatomic Distances and Bond Angles for $(\eta^5\text{-}C_5Me_5)_2Mo_2Fe_2(CO)_9(\mu_2\text{-}CO)(\eta^2,\mu_4\text{-}CO)\cdot C_7H_8$

A. Interatomic Distances (Å)

Mo(1)-Fe(1)	2.862 (5)	C(1)-O(1)	1.12 (4)
Mo(1)-Fe(2)	2.800 (6)	C(2)-O(2)	1.23 (4)
Mo(2)-Fe(1)	2.882 (6)	C(3)-O(3)	1.24 (5)
Mo(2)-Fe(2)	2.719 (6)	C(4)-O(4)	1.10 (4)
Fe(1)-Fe(2)	2.548 (8)	C(5)-O(5)	1.08 (4)
Mo(1)-C	2.06 (4)	C(6)-O(6)	1.16 (4)
Mo(2)-C	2.54 (4)	C(7)-O(7)	1.10 (4)
Mo(2)-O	2.15 (2)	C(8)-O(8)	1.26 (4)
Fe(1)-C	2.25 (5)	C(9)-O(9)	1.19 (4)
Fe(2)-C	2.19 (4)	C(10)-O(10)	1.21 (5)
C-O	1.19 (4)	Mo(1)-Cp(1)	2.40 (3)
Mo(1)-C(1)	1.94 (4)	Mo(1)-Cp(2)	2.32 (3)
Mo(1)-C(2)	1.92 (3)	Mo(1)-Cp(3)	2.33 (2)
Mo(2)-C(6)	1.98 (4)	Mo(1)-Cp(4)	2.42 (3)
Mo(2)-C(7)	1.98 (4)	Mo(1)-Cp(5)	2.46 (2)
Fe(1)-C(3)	1.74 (4)	Mo(2)-Cp(6)	2.28 (3)
Fe(1)-C(4)	1.79 (4)	Mo(2)-Cp(7)	2.25 (2)
Fe(1)-C(5)	1.74 (4)	Mo(2)-Cp(8)	2.36 (2)
Fe(2)-C(8)	1.64 (4)	Mo(2)-Cp(9)	2.45 (2)
Fe(2)-C(10)	1.71 (4)	Mo(2)-Cp(10)	2.41 (2)
Fe(1)-C(9)	2.12 (4)		
Fe(2)-C(9)	1.88 (4)		
Fe(2)-C(7)	2.46 (4)		

B. Bond Angles (deg)

Fe(1)-Mo(1)-Fe(2)	53.5 (2)	Mo(1)-C-Mo(2)	148 (2)
Fe(1)-Mo(2)-Fe(2)	54.0 (2)	Fe(1)-C-Fe(2)	70 (2)
Mo(1)-Fe(1)-Mo(2)	100.8 (2)	Mo(1)-C-Fe(1)	83 (2)
Mo(1)-Fe(2)-Mo(2)	106.7 (2)	Mo(1)-C-Fe(2)	82 (2)
Mo(1)-Fe(1)-Fe(2)	62.0 (2)	Mo(2)-C-Fe(1)	74 (1)
Mo(1)-Fe(2)-Fe(1)	64.5 (2)	Mo(2)-C-Fe(2)	70 (1)
Mo(2)-Fe(1)-Fe(2)	59.7 (2)	Mo(1)-C-O	154 (4)
Mo(2)-Fe(2)-Fe(1)	66.3 (2)	Mo(2)-C-O	58 (2)
Fe(1)-C-O	117 (3)	Mo(2)-O-C	94 (3)
Fe(2)-C-O	119 (3)		

$R_1(F)$ and $R_2(F)$ values which were 0.3 and 0.4% higher, respectively, than the original ones. Hence, the results reported here are for the original least-squares refinement.

Positional parameters for the nonhydrogen atoms from the last full-matrix least-squares cycle are presented in Table II. Interatomic distances and bond angles are given in Table III. Tables of idealized coordinates for the hydrogen atoms, temperature factors for all atoms, and a listing of the observed and calculated structure factor amplitudes are available as supplementary material.

Results and Discussion

Crystal Structure of $(\eta^5\text{-}C_5Me_5)_2Mo_2Fe_2(CO)_9(\mu_2\text{-}CO)(\eta^2,\mu_4\text{-}CO)\cdot C_7H_8$ (1-tol). The solid-state structure is composed of well-separated discrete molecules. There is no evidence of abnormal packing forces that would produce marked geometrical distortions of the crystallographically independent molecule, for which ORTEP views are shown in Figures 5 and 6. The cluster core of 1 consists of a butterfly arrangement of metal atoms with the two iron atoms occupying the hinge positions and the two molybdenum atoms located at the wingtip positions. The most striking feature of this cluster is the unusual η^2 linkage of the bridging carbonyl ligand to the butterfly Mo_2Fe_2 core (vide infra).

During the latter stages of the structural refinement of 1·tol, we found that the thermal parameters of several of the carbonyl ligands became nonpositive definite when attempts were made to change from isotropic to anisotropic thermal models. Furthermore, there appeared to be localized regions of residual electron density located near some of the carbonyl carbon and/or oxygen atoms. Data collected from three different crystals (prepared from three different reactions) exhibited the same problems upon refinement regardless of whether the intensity data were collected with either θ–2θ scans or ω scans and independent of whether an empirical or analytical absorption correction was applied. There was no evidence for problems arising from extinction or double reflections in any of the data sets. No stacking faults were noted, and no evidence of twinning was indicated from the axial photographs.

We interpret these observations as being consistent with a crystal-disorder phenomenon in which there are presumably at least two forms of 1 which differ slightly in the disposition of their carbonyl ligands. While we were not able to satisfactorily model this crystal disorder, we have been able to obtain a meaningful structural determination by conducting the refinement with isotropic temperature factors for the carbonyl ligands and anisotropic thermal parameters for the metal atoms; the $(\eta^5\text{-}C_5Me_5)$ groups were refined as rigid groups with a TLX model. Although a relatively precise measurement of the positional and thermal parameters for the carbonyl ligands is precluded by the ligand disorder in 1, the overall configuration consisting of the butterfly metal core with a π-bound carbonyl ligand is unambiguously established and is in complete accordance with the spectroscopic measurements.

Stereochemical Relationship of the Tetrametal $(\eta^2,\mu_4\text{-}CO)$ Cores in $(\eta^5\text{-}C_5Me_5)_2Mo_2Fe_2(CO)_9(\mu_2\text{-}CO)(\eta^2,\mu_4\text{-}CO)$ (1) and Other Clusters and Resulting Bonding Implications. (a) Two $[Fe_4(CO)_{12}(\mu_2\text{-}X)(\eta^2,\mu_4\text{-}CO)]^-$ Monoanions (X = H (2); X = $AuPEt_3$ (3)). An examination of the solid-state architectures of 1 and two butterfly tetrairon isomers, 2[11a] and 3[13], reveals geometrical similarities and differences. 2 and 3 are structurally analogous with crystallographic and pseudo C_s—m site symmetry, respectively, such that the η^2-carbonyl ligand is symmetrically bonded to the butterfly Fe_4 core which has essentially equivalent Fe–Fe distances that average 2.627 Å in 2 and 2.642 Å in 3. In contrast, the butterfly Mo_2Fe_2 core in 1 is distorted from C_s—m geometry, as evidenced by the different single-bond Mo(1)–Fe(1) and Mo(1)–Fe(2) distances of 2.862 (5) and 2.800 (6) Å, respectively, and the different Mo(2)–Fe(1) and Mo(2)–Fe(2) distances of 2.882 (6) and 2.719 (6) Å, respectively. The fact that the two longer Mo–Fe electron-pair bonds are associated with Fe(1) and the two shorter Mo–Fe ones with Fe(2) is not surprising because Fe(1) is coordinated to one more terminal carbonyl group than Fe(2). The carbonyl-bridged Fe(1)–Fe(2) hinge bond in 1 measures 2.548 (8) Å, which is considerably shorter than the corresponding H-bridged Fe–Fe hinge bond of 2.620 (5) Å in 2 and the Au_3PEt_3-bridged Fe–Fe hinge bond of 2.649 (2) Å in 3. These bond-length variations are consistent with previous observations that a bridging carbonyl ligand normally causes a shortening of a metal–metal bond whereas a single, unsupported bridging hydride ligand normally causes a lengthening of a metal–metal bond.[36]

A salient structural feature of 1 is the disposition of the π-bound carbonyl ligand within the edge-opened Mo_2Fe_2 tetrahedron (Figures 5 and 6). Linkage of the capping carbonyl carbon atom to the Mo(1)Fe(1)Fe(2) triangle gives rise to an unusually short Mo(1)–C distance of 2.06 (4) Å and longer Fe(1)–C and Fe(2)–C distances of 2.25 (5) and 2.19 (4) Å, respectively. The η^2 attachment of the carbonyl ligand to the wingtip Mo(2) atom results in Mo(2)–C and Mo(2)–O distances of 2.54 (4) and 2.15 (2) Å, respectively, and a C–O distance of 1.19 (4) Å. For the more precisely determined structure of 3,[13] the capping carbonyl carbon is also much closer to the one wingtip iron atom (1.851 (9) Å) than to the two mirror-related hinge iron atoms (2.082

(36) (a) Dahl, L. F. In *Anal. N. Y. Acad. Sci.* **1984**, 1–26. (b) Churchill, M. R.; DeBoer, B. G.; Rotella, F. J. *Inorg. Chem.* **1976**, *15*, 1843–1853 and references cited therein.

(6) Å). The Fe–C and Fe–O distances for the other wingtip iron atom π-coordinated to the carbonyl ligand are 2.137 (9) and 1.996 (5) Å, respectively, while the elongated C–O bond length is 1.254 (9) Å.

Especially noteworthy is that the carbonyl oxygen atom is closer than the carbonyl carbon atom to the π-coordinated wingtip metal atom by 0.39 Å in **1** and by 0.14 Å in **3**. We suggest that this particular bond-length variation has an electronic origin which supports the premise that the η^2-coordinated carbonyl ligand is a π-donor rather than a π^*-acceptor in its bonding interaction with the wingtip metal atom in **1**, **2**, and **3**. These electronic considerations are based upon the filled, orthogonal 1π MO's of carbon monoxide having considerably greater oxygen orbital character and the empty, orthogonal 2π (or π^*) MO's of carbon monoxide possessing much larger carbon orbital character. In the case where the π-donating interaction of an η^2-CO ligand energetically dominates over the corresponding π^*-acceptor interaction with a metal atom, one would expect (in the absence of an abnormal steric influence) the oxygen atom to be positioned nearer to the π-coordinated metal atom. Hence, the observed geometries of the tetrametal (η^2,μ_4-CO) cores of **1**, **2**, and **3** point to the π-bound CO ligand acting as a four-electron donor in agreement with electron-counting rules[37] which normally require a 62-electron count for a butterfly metal geometry.

(b) $(\eta^5\text{-}C_5H_5)_2Mo_2Co_2(\eta^5\text{-}C_5Me_5)_2(\mu_2\text{-}CO)_3(\eta^2,\mu_4\text{-}CO)$. In this unique example, an η^2,μ_4- carbonyl ligand is coordinated to a different kind of tetrametal fragment. An X-ray diffraction study by Stone and co-workers[38] revealed that this cluster of crystallographic mirror-plane symmetry has a Mo_2Co_2 framework made up of a completely bonding isosceles $MoCo_2$ triangle attached to a second Mo atom by a presumed Mo–Mo double bond (2.574 (1) Å) oriented nearly perpendicular to the $MoCo_2$ plane. The η^2-carbonyl ligand is bound to the Mo_2Co_2 fragment such that the C–O bond is essentially perpendicular (as a triply bridging ligand) to the $MoCo_2$ triangle. A bonding model consistent with the observed molecular parameters and electron-counting rules emerges if one considers the η^2-carbonyl ligand to be a six-electron donor in which the filled carbon-based 5σ(CO) MO is involved in a multicentered two-electron bond to the $MoCo_2$ triangle while the two filled, orthogonal 1π(CO) MO's are each involved in a multicentered two-electron bond mainly to the out-of-plane molybdenum atom. This consideration of the carbonyl ligand as a six-electron donor leads to an observed electron count of 62 valence electrons which is that predicted for a tetrametal cluster possessing an electron-precise tetrahedral metal architecture with one double-bond edge, three single-bond edges, and two "open" no-bond edges. Its bonding formulation as a four-electron π-donor (instead of a π^*-acceptor) of electron charge is also consistent with the carbonyl oxygen atom being 0.32 Å closer than the carbonyl carbon atom to the out-of-plane π-coordinated Mo atom. This particular geometrical arrangement was viewed by Stone and co-workers[38] as a molecular model for carbon monoxide activation on a stepped metal surface.[39] They also pointed out that crystallographic evidence for the substantial activation of this C–O bond is given by its long bond length of 1.283 (3) Å which is similar to that of 1.303 (14) Å observed by Herrmann et al.[40] for the presumed six-electron-donating η^2-carbonyl ligand in the 48-electron *triangulo*-Nb_3 cluster, $(Nb_3(\eta^5\text{-}C_5H_5)_3(CO)_6(\eta^2(\mu_3\text{-}C,\mu_2\text{-}O)\text{-}CO)$.[41,42]

Scheme I

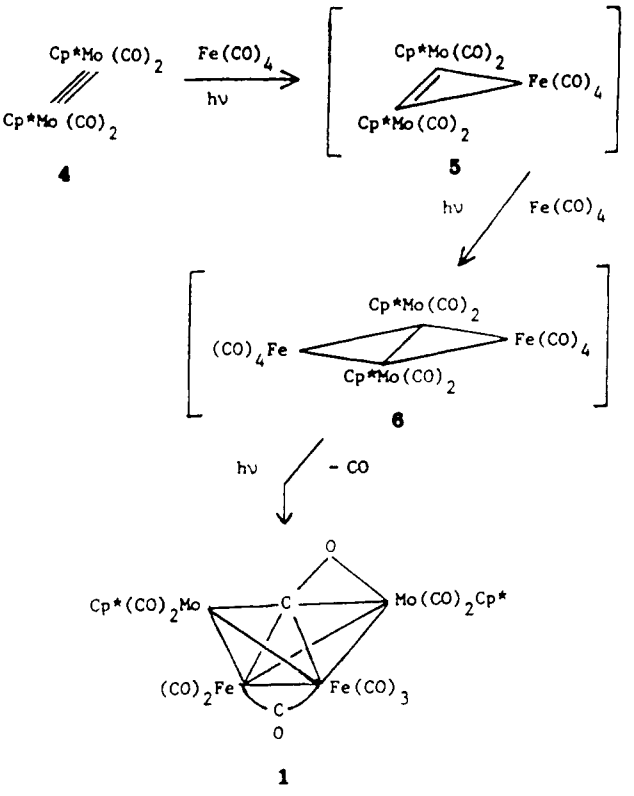

Synthesis of $(\eta^5\text{-}C_5Me_5)_2Mo_2Fe_2(CO)_9(\mu_2\text{-}CO)(\eta^2,\mu_4\text{-}CO)$. Reaction of the inorganic acetylene analogue (**4**) with photolytically generated methylene-like $Fe(CO)_4$ fragment(s) was attempted in order to obtain a dimolybdenum–iron cyclopropene-like cluster and/or a dimolybdenum–diiron bicyclobutane-like cluster (Scheme I). While there would appear to be little relation between the predicted bicyclobutane-like 62-electron **6** and the isolated 62-electron **1**, one can readily envision the photolytic conversion of **6** into **1** by the following sequence: (1) a photoinduced loss of a carbonyl ligand from one of the iron atoms of **6**; (2) formation of an Fe–Fe bond and concomitant cleavage of the Mo–Mo bond; (3) insertion of one of the iron-bound carbonyl ligands into the edge-opened Mo_2Fe_2 tetrahedron to give a four-electron-donating η^2-carbonyl group along with the formation of a hinge-bridging carbonyl group across the Fe–Fe bond. In connection with the second step, the edge-opened tetrahedral (butterfly) tetraplatinum cores in the 58-electron $Pt_4L_4(\mu_2\text{-}CO)_5$ clusters (L = PEt_3, PMe_2Ph, $PMePh_2$, PEt_2-*t*-Bu) exhibit variable-temperature multinuclear spectra consistent with rapid interconversion of the two

(37) (a) Lauher, J. W. *J. Am. Chem. Soc.* **1978**, *100*, 5305–5315. (b) Mingos, D. M. P. *Chem. Soc. Rev.* **1986**, *15*, 31–61 and references cited therein. (c) Teo, B. K.; Longoni, G.; Chung, F. R. K. *Inorg. Chem.* **1984**, *23*, 1257–1266 and references cited therein. (d) Tachikawa, M.; Muetterties, E. L. *Prog. Inorg. Chem.* **1981**, *28*, 203–238. (e) Gladfelter, W. L. *Adv. Organomet. Chem.* **1985**, *24*, 41–86.

(38) Brun, P.; Dawkins, G. M.; Green, M.; Miles, A. D.; Orpen, A. G.; Stone, F. G. A. *J. Chem. Soc., Chem. Commun.* **1982**, 926–927.

(39) Muetterties, E. L.; Rhodin, T. N.; Band, E.; Brucker, C. F.; Pretzer, W. R. *Chem. Rev.* **1979**, *79*, 91–137 and references cited therein.

(40) (a) Herrmann, W. A.; Biersack, H.; Ziegler, M. L.; Weidenhammer, K.; Siegel, R.; Rehder, D. *J. Am. Chem. Soc.* **1981**, *103*, 1692–1699. (b) Herrmann, W. A.; Ziegler, M. L.; Weidenhammer, K.; Biersack, H. *Angew. Chem., Int. Ed. Engl.* **1979**, 960–962.

(41) The mobility of the six-electron-donating η^2-carbonyl ligand, which has a low-frequency absorption band at 1330 cm^{-1} only in the solid state,[42] was analyzed by Lewis and Caulton[42] from a variable-temperature ^1H NMR study of $Nb_3(\eta^5\text{-}C_5H_5)_3(CO)_6(\eta^2(\mu_3\text{-}C,\mu_2\text{-}O)\text{-}CO)$ and its methylcyclopentadienyl-substituted analogue.

(42) Caulton, K. G.; Lewis, L. N. *Inorg. Chem.* **1980**, *19*, 3201–3203.

wingtip Pt atoms and two hinge Pt atoms via concerted Pt–Pt bond breaking and bond making.[43] Attempts to synthesize **6** by bubbling carbon monoxide through a solution of **1** were unsuccessful; in all cases the products isolated were $Mo_2(\eta^5\text{-}C_5Me_5)_2(CO)_6$ and iron pentacarbonyl.

Variable-temperature multinuclear NMR studies by Horwitz and Shriver[12-14] have shown that a solution of each of the $[Fe_4(CO)_{12}(\mu_2\text{-}X)(\eta^2,\mu_4\text{-}CO)]^-$ monoanions (X = H (**2**); X = $AuPEt_3$ (**3**); X = CuL (where L = PPh_3, $CNC_6H_3Me_2$-2,6); X = HgMe) actually consists of an equilibrium mixture of two geometrical isomers—viz., the 62-electron monoanion containing the butterfly $Fe_4(\eta^2,\mu_4\text{-}CO)$ core with a hinge-bridging Lewis acid $(\mu_2\text{-}X)^+$ ligand and the 60-electron monoanion containing a closed Fe_4 core with a face-capping $(\mu_3\text{-}X)^+$ ligand. Crystallization of both isomers of the $[AuPEt_3]^+$ adduct with different counterions as well as the variable-temperature NMR data were interpreted[12-14] as being indicative of a small energy difference between the two isomers. We find no evidence of interconversion between the observed butterfly Mo_2Fe_2 form of **1** and a corresponding closed tetrahedral Mo_2Fe_2 form.

The original conversion by protonation of the "closed" tetrahedral $[Fe_4(CO)_{12}(\mu_3\text{-}CO)]^{2-}$ dianion to the "open" butterfly monoanion (**2**) containing a π-coordinated CO ligand was attributed to increased steric demands resulting from the addition of another ligand.[11a] However, initial attempts by Horwitz and Shriver[44] to synthesize butterfly metal clusters containing π-bound carbonyl ligands by the preparation of highly crowded tetrahedral metal clusters were unsuccessful; the structure of the resulting $[Fe_3M(CO)_{14}]^{2-}$ dianions (M = Cr, Mo, W) exhibited 0.1-Å enlarged Fe–Fe distances consistent with the increased strain energy being relieved by an enlargement of the metal core. Subsequently, Horwitz and Shriver[13,14] reacted other Lewis acids with the $[Fe_4(CO)_{12}(\mu_3\text{-}CO)]^{2-}$ dianion to isolate the desired tetrairon monoanions with π-bound carbonyl ligands (vide supra). For the corresponding "closed" tetrahedral iron isomers, relief of increased steric strain was again accomplished by an increase of the metal–metal distances within the cluster.[13] We believe that steric forces may play an important role in inducing the conversion of a "closed" 60-electron tetrahedral metal cluster to an open 62-electron butterfly metal cluster with a π-bound CO ligand. The large size and relative immobility of the $\eta^5\text{-}C_5Me_5$ ligands in **1** would likely impart considerable strain to any Mo–Mo bond present in a "closed" tetrahedral Mo_2Fe_2 precursor of **1**.

Under O_2-free conditions, the photolytic reaction of $Fe_2(CO)_9$ with **4** yields **1** as the only mixed-metal product. Some $Fe(CO)_5$ was also isolated along with $Mo_2(\eta^5\text{-}C_5Me_5)_2(CO)_6$ which is formed from the reaction of liberated CO with **4**.[45] Our attempts to synthesize the sought-after cyclopropene- or bicyclobutane-like clusters (**5** and **6**) by thermal reactions between $Fe_2(CO)_9$ and **4** or between $Fe(CO)_4(NC_5H_5)$ and **4** have thus far been unsuccessful. Neither have we succeeded in synthesizing the tungsten analogue of **1** by reacting $Fe_2(CO)_9$ with $W_2(\eta^5\text{-}C_5Me_5)_2(CO)_4$. A substitution of $Fe(CO)_5$ or $Fe_3(CO)_{12}$ for $Fe_2(CO)_9$ and/or $Mo_2(\eta^5\text{-}C_5Me_5)_2(CO)_6$ for **4** gave rise to the same final product (**1**). In all cases in which $Mo_2(\eta^5\text{-}C_5Me_5)_2(CO)_6$ was used as a reagent, we noted no obvious reaction between the iron carbonyl and molybdenum dimer until a substantial portion of $Mo_2(\eta^5\text{-}C_5Me_5)_2(CO)_6$ had been photodecarbonylated to **4** (as evidenced by infrared spectra taken during the course of the reaction). Infrared spectra taken during the photolytic reaction of **4** with an excess of $Fe(CO)_5$ indicated that the $Fe(CO)_5$ was initially converted to $Fe_2(CO)_9$ with the concomitant reaction of **4** with liberated CO to form $Mo_2(\eta^5\text{-}C_5Me_5)_2(CO)_6$.

Characterization of $(\eta^5\text{-}C_5Me_5)_2Mo_2Fe_2(CO)_9(\mu_2\text{-}CO)(\eta^2,\mu_4\text{-}CO)$ (1). (a) Spectroscopic Properties. In accordance with its solid-state structure, an infrared spectrum of **1** in C_6H_6 (Figure 1, supplementary material) displays several carbonyl stretching bands in the terminal carbonyl region between 1895 and 2030 cm^{-1}, a weak band in the doubly bridging carbonyl region at 1829 cm^{-1}, as well as bands at 1380 and 1340 cm^{-1}. The peak at 1380 cm^{-1} is assigned to the asymmetric ring breathing mode of the $(\eta^5\text{-}C_5Me_5)$ ligands and is consistent with the observation that a band of roughly the same intensity is located at 1380 $\pm$ 10 cm^{-1} in all of the $(\eta^5\text{-}C_5Me_5)$-containing molybdenum complexes that we have examined.[9,10] The band at 1340 cm^{-1} is assigned to the activated π-bound carbonyl ligand, since incorporation of ^{13}CO into the cluster results in the appearance of a new peak at 1330 cm^{-1}. A solid-state infrared spectrum shows much the same features except that the absorbances are considerably broader. The very low carbonyl stretching frequency in **1**, which was found to be 1338 cm^{-1} in the solid state, is comparable to similarly low frequencies in **2** (1415 cm^{-1} for the $[PPN]^+$ salt and 1382 cm^{-1} for the K^+ salt in the solid state) and in **3** (1412 cm^{-1} in the solid state as the $[K(18\text{-crown-}6)]^+$ salt).[13,14]

Proton NMR spectra (C_6D_6) of **1**·tol are consistent with the solid-state structure being retained in solution; two sharp, equally intense resonances observed at δ 1.59 and 1.69 are assigned to the two chemically nonequivalent $(\eta^5\text{-}C_5Me_5)$ ligands. Resonances attributable to the toluene molecule were also observed. The sharpness of these ^1H NMR resonances provides definitive evidence for the predicted dimagnetism of **1**. Room-temperature ^{13}C NMR spectra of **1** (either natural abundance or 12% ^{13}CO-enriched) in CD_2Cl_2 exhibited a single, very broad resonance at δ 227 which is assigned to the average of all of the carbonyl ligands which evidently are fluxional on the NMR time scale. At −60 °C, sharp resonances of relative intensities 1:1:1:2 are observed at δ 274.0, 241.4, 232.4, and 226.1 with an additional broad resonance of relative intensity 6 located at δ 216.3 (Figure 2, supplementary material). The low-field resonance (δ 274.0) is assigned to the π-bound CO ligand and is similar to the reported chemical shifts for the analogous ligand in **2** (δ 279.7)[12] and **3** (δ 284.6).[13,14] The resonances of equal intensities located at δ 241.4 and 232.4 are assigned to the two nonequivalent carbonyl ligands of one of the wingtip molybdenum atoms. The larger resonance at δ 226.1 is assigned to the two remaining Mo-coordinated carbonyl ligands which are equivalent on the NMR time scale. The broad resonance located at δ 216.3 is assigned to the six iron-coordinated carbonyl ligands which appear to be exchanging rapidly even at −60 °C.

(b) Chemical Properties. The butterfly **1** crystallizes from toluene to give relatively air-stable black needle-like crystals of **1**·tol, which are soluble in common organic solvents to give moderately air-stable brown solutions. Cyclic voltammetric measurements of solutions of **1** in CH_2Cl_2 (Figure 3, supplementary material) revealed a single quasi-reversible redox couple centered at an $E_{1/2}$ value of 0.568 V vs SCE (ΔE_p = 81 mV); this couple was shown by an electrolysis experiment to represent an oxidation process. Reaction of a stirred solution of **1** with an

(43) Pregosin, P. S.; Venanzi, L. M.; Welch, A. J. *Inorg. Chim. Acta* **1984**, *85*, 103–110.
(44) Horwitz, C. P.; Holt, E. M.; Shriver, D. F. *Inorg. Chem.* **1984**, *23*, 2491–2499.
(45) Ginley, D. S.; Wrighton, M. S. *J. Am. Chem. Soc.* **1975**, *97*, 3533–3535.

equimolar quantity of $AgPF_6$ resulted in the formation of a grayish precipitate as well as what is presumably the oxidized form of **1**. The oxidized species decomposes rapidly in solution to give an insoluble yellowish brown material and an unidentified soluble brown material.

The chemistry of the butterfly tetrairon **2** has been extensively studied by Shriver and co-workers.[12,18-20] Protonation of **2** at −90 °C was found to occur at the oxygen atom of the π-bound carbonyl ligand, as judged by the appearance in a proton NMR spectrum of a characteristic low-field resonance at δ 13.2 as well as by ^{13}C NMR evidence.[12] The protonated species is unstable at higher temperatures and decomposes with C–O bond cleavage[18-20,46] to give $Fe_4(CO)_{12}(\mu_2\text{-}H)(\eta^2,\mu_4\text{-}CH)$.[47] Earlier independent studies by both Whitmire, Shriver, and Holt[19a] and Lewis, Johnson, and co-workers[48] showed that protonation of the oxygen-methylated 60-electron $[Fe_4(CO_{12}(\mu_3\text{-}COMe)]^-$ monoanion[46,48,49] produces the corresponding 62-electron $Fe_4(CO)_{12}(\mu_2\text{-}H)(\eta^2,\mu_4\text{-}COMe)$ molecule containing an $Fe_4(\eta^2,\mu_4\text{-}COMe)$ core; the Lewis–Johnson group[48] also reported that this compound could be prepared by methylation of the $[Fe_4(CO)_{12}(\mu_2\text{-}H)(\eta^2,\mu_4\text{-}CO)]^-$ monoanion with $[Me_3O]^+[BF_4]^-$.

We have found no evidence for the reaction of **1** with triflic acid. When a sample of **1** was mixed with a slight excess of HSO_3CF_3 at 20 °C, the ^1H NMR peaks due to the $(\eta^5\text{-}C_5Me_5)$ ligands did not shift. No new ^1H NMR resonances were observed in the range of +20 to −20 ppm. A comparison of the integrated intensities of the ^1H NMR resonances due to **1** and the resonance due to residual solvent protons indicated that (within experimental error) none of the starting cluster had reacted with the triflic acid. Attempts to react **1** with a slight excess of $MeSO_3CF_3$ at 20 °C were also unsuccessful.

The marked difference in the protonation reactivities of **1** and **2** can be attributed (at least in part) to a charge effect, with the anionic **2** being intrinsically more susceptible to electrophilic attack than the neutral **1**. Molecular orbital calculations performed[50] on **2** indicate that the highest occupied molecular orbitals are localized to a large extent at a sterically accessible site on a wingtip metal atom. The coordination of a proton to **2** at such a site would require little reorganization of the terminally bound carbonyl ligands. Migration of the proton to the π-bound carbonyl ligand would give the reported $Fe_4(CO)_{12}(\mu_2\text{-}H)(\eta^2,\mu_4\text{-}COH)$[12] which was proposed as an intermediate prior to C–O bond scission on the basis of the known structure of the corresponding O-methylated analogue.[48,49] While there is no reason to assume that the HOMO of **1** is similarly localized on a wingtip metal atom, we note that protonation at such a site should be inhibited by the steric bulk of the $\eta^5\text{-}C_5Me_5$ ligand. Furthermore, the presence of these relatively immobile ligands would be expected to result in a rather large barrier for protonation and concomitant carbonyl-ligand reorganization.

Structural Model for Dinitrogen Fixation in Nitrogenase. On the basis of the observed geometry of the $Mo_2Fe_2(\eta^2,\mu_4\text{-}CO)$ core of **1**, we hereby propose that a reasonable structural model for the active site of the dinitrogen-fixing enzyme nitrogenase[51] (which contains a Mo–Fe protein with two cores each composed of one Mo and six to eight Fe atoms) involves the isoelectronic dinitrogen molecule being π-bonded to a wingtip molybdenum atom in an enclosed butterfly $MoFe_3$ cavity. One attractive feature of this model is that it provides a plausible mechanism for capturing a N_2 molecule and for an activation of its triple bond by interaction of one of its two π bonds with a wingtip molybdenum atom. A rupturing of a Mo–Fe bond edge of a completely bonding tetrahedral $MoFe_3$ fragment (viewed as the resting state) to give a butterfly tetrametal geometry allows the N_2 molecule in either the free or monodentate form to become tetrametal-coordinated as a four-electron donor. The proton-induced six-electron reduction of the coordinated dinitrogen molecule to two ammonia molecules is presumed to involve an initial protonation of the exposed nitrogen atom followed by reductive N–N bond cleavage to give one ammonia molecule and an intermediate butterfly $MoFe_3(\mu_4\text{-}N)$ fragment of an iron–molybdenum core. Subsequent protonation–reduction is then presumed to convert the tetrametal-coordinated nitride atom to ammonia.

Analyses[52] of Mo and Fe EXAFS spectra performed on the iron–molybdenum cofactor (FeMo-co) of nitrogenase have led to Mo–Fe distances of 2.75 and 3.5 Å and to Fe–Fe distances of 2.66 Å. These data also indicate Mo–(light atom) (viz., C, N, or O) bond lengths of 1.8 and 2.1 Å and Fe–(light atom) bond lengths of 1.8 Å. For a hypothetical $MoFe_3(\eta^2,\mu_4\text{-}N_2)$ butterfly-like fragment which is proposed to correspond to the active site of nitrogenase, estimated distances based on those determined for the $Mo_2Fe_2(\eta^2,\mu_4\text{-}CO)$ core in **1** and for the $Fe_4(\eta^2,\mu_4\text{-}CO)$ core in **2** are in accordance with the above distances obtained from the EXAFS measurements on FeMo-co.

Acknowledgment. Support of this research by the National Science Foundation is gratefully appreciated. Professor A. David Rae is thanked for his helpful advice concerning the crystallographic aspects of this project.

Registry No. **1**, 111847-27-9; **1**·tol, 111847-28-0; **3**, 12132-04-6; $Fe_2(CO)_9$, 15321-51-4; $Mo_2(\eta^5\text{-}C_5Me_5)_2(CO)_6$, 56200-14-7; nitrogenase, 9013-04-1; Fe, 7439-89-6; Mo, 7439-98-7.

Supplementary Material Available: Figure 1 displays a solution IR spectrum of $(\eta^5\text{-}C_5Me_5)_2Mo_2Fe_2(CO)_9(\mu_2\text{-}CO)(\eta^2,\mu_4\text{-}CO)$

(46) Holt, E. M.; Whitmire, K. H.; Shriver, D. F. *J. Am. Chem. Soc.* **1982**, *104*, 5621–5626.
(47) (a) Tachikawa, M.; Muetterties, E. L. *J. Am. Chem. Soc.* **1980**, *102*, 4541–4542. (b) Beno, M. A.; Williams, J. M.; Tachikawa, M.; Muetterties, E. L. *J. Am. Chem. Soc.* **1980**, *102*, 4542–4544; **1981**, *103*, 1485–1492.
(48) Dawson, P. A.; Johnson, B. F. G.; Lewis, J.; Raithby, P. R. *J. Chem. Soc., Chem. Commun.* **1980**, 781–783.
(49) Holt, E. M.; Whitmire, K.; Shriver, D. F. *J. Chem. Soc., Chem. Commun.* **1980**, 778–779.
(50) Fehlner, T. P.; Housecroft, C. E. *Organometallics* **1984**, *3*, 764–774.
(51) For recent proposals pertaining to models of the active site in the iron–molybdenum cofactor, FeMoco, of nitrogenase, see: (a) Averill, B. A. *Struct. Bonding (Berlin)* **1983**, *53*, 59–103 and references cited therein. (b) Holm, R. H. *Chem. Soc. Rev.* **1981**, *10*, 455–490 and references cited therein. (c) Teo, B.-K. In *New Frontiers in Organo-metallic and Inorganic Chemistry*; Yaozeng, H., Yamamoto, A., Teo, B.-K., Eds.; Science Press: Beijing, The People's Republic of China, 1984; pp 341–352, and references cited therein. (d) Kanatzidis, M. G.; Coucouvanis, D. *J. Am. Chem. Soc.* **1986**, *108*, 337–338 and references cited therein. (e) Walters, M. A.; Chapman, S. K.; Orme-Johnson, W. H. *Polyhedron* **1986**, *5*, 561–565. (f) Newton, W. E.; Schultz, F. A.; Gheller, S. F.; Lough, S.; McDonald, J. W. *Polyhedron* **1986**, *5*, 567–572 and references therein.
(52) (a) Cramer, S. P. Eccles, T. K.; Kutzler, F. W.; Hodgson, K. O.; Mortenson, L. E. *J. Am. Chem. Soc.* **1976**, *98*, 1287–1288. (b) Cramer, S. P.; Hodgson, K. O.; Gillum, W. O.; Mortenson, L. E. *J. Am. Chem. Soc.* **1978**, *100*, 3398–3407. (c) Cramer, S. P.; Gillum, W. O.; Hodgson, K. O.; Mortenson, L. E.; Stiefel, E. I.; Chisnell, J. R.; Brill, W. J.; Shah, V. K. *J. Am. Chem. Soc.* **1978**, *100*, 3814–3819. (d) Antonio, M. R.; Teo, B.-K.; Orme-Johnson, W. H.; Nelson, M. J.; Groh, S. E.; Lindahl, P. A.; Kauzlarich, S. M.; Averill, B. A. *J. Am. Chem. Soc.* **1982**, *104*, 4703–4705. (e) Burgess, B. K.; Yang, S.-S.; You, C.-B.; Li, J.-G.; Friesen, G. B.; Pan, W.-H.; Stiefel, E. I.; Newton, W. E.; Conradson, S. D.; Hodgson, K. O., In *Current Perspectives in Nitrogen Fixation*: Gibson, A. H., Newton, W. E., Eds.; Elsiver-North Holland: Amsterdam, 1981; p 71. (f) Newton, W. E.; Burgess, B. K.; Cummings, S. C.; Lough, S.; McDonald, J. W.; Rubinson, J. F.; Conradson, S. D. Hodgson, K. O. In *Advances in Nitrogen Fixation Research*; Veeger, C., Newton, W. E., Eds.; Martinus Nijhoff: The Hague, 1984; p 160.

(1), Figure 2 presents a low-temperature ^{13}C NMR spectrum of 1, Figure 3 shows a cyclic voltammogram of 1, Figure 4 shows the two relative orientations of the disordered toluene molecule found in the solid-state structure of 1·tol, tables of idealized coordinates for the hydrogen atoms and thermal parameters for all atoms for 1·tol (6 pages); a listing of the observed and calculated structure factor amplitudes for 1·tol (20 pages). Ordering information is given on any current masthead page.

Molybdenum-Promoted Nitrosyl Bond Activation: Synthesis and Characterization of $(\eta^5\text{-}C_5Me_5)_3Mo_3Co_2(CO)_8(\mu_3\text{-}NH)(\mu_4\text{-}N)$, an Unusual Mixed-Metal Cluster Containing Tetrametal-Coordinated Nitrido and Trimetal-Coordinated Imido Ligands, and of $(\eta^5\text{-}C_5Me_5)_2Mo_2Co_3(CO)_{10}(\mu_5\text{-}N)$, a 74-Electron Square-Pyramidal Mixed-Metal Cluster Containing a Pentametal-Coordinated Nitrido Ligand

Charles P. Gibson[1] and Lawrence F. Dahl*

Department of Chemistry, University of Wisconsin—Madison, Madison, Wisconsin 53706

Received September 15, 1986

An attempt to provide a new synthetic route to ON-capped metal clusters (which are relatively rare) via cycloaddition of a photolytically generated metal nitrosyl fragment to the Mo–Mo triple-bonded $Mo_2(\eta^5\text{-}C_5Me_5)_2(CO)_4$ dimer has led instead to Mo-promoted N–O bond cleavage to give two unusual nitrido-containing metal clusters—viz., $(\eta^5\text{-}C_5Me_5)_3Mo_3Co_2(CO)_8(\mu_3\text{-}NH)(\mu_4\text{-}N)$ (1) as a major mixed-metal product (11% yield) and $(\eta^5\text{-}C_5Me_5)_2Mo_2Co_3(CO)_{10}(\mu_5\text{-}N)$ (2) as a minor product (<1% yield). Other major products from the photolytic reaction of $Co(CO)_3NO$ with the 30-electron $Mo_2(\eta^5\text{-}C_5Me_5)_2(CO)_4$ in THF were $Mo(\eta^5\text{-}C_5Me_5)(CO)_2NO$ and $Mo_2(\eta^5\text{-}C_5Me_5)_2(CO)_6$. Elemental, spectroscopic (IR and ^1H and ^{15}N NMR), and single-crystal X-ray diffraction analyses established that 1 possesses a butterfly $Mo_2Co_2(\mu_4\text{-}N)$ core composed of two backbone Co and two wingtip Mo atoms coordinated to a five-electron-donating N atom. This "edge-opened" tetrahedral metal fragment may be viewed as an electron-precise, 62-electron system in which the Co and Mo atoms of one bonding Co–Mo edge are each linked by additional electron-pair bonds to the Mo and N atoms of a five-electron-donating $Mo(\eta^5\text{-}C_5Me_5)(CO)_2NH$ fragment. The edge-fusion of the resulting "closed" tetrahedral $Mo_2Co(\mu_3\text{-}NH)$ system to the central butterfly $Mo_2Co_2(\mu_4\text{-}N)$ core produces an overall $Mo_3Co_2(\mu_3\text{-}NH)(\mu_4\text{-}N)$ cluster which is encapsulated by three Mo-coordinated C_5Me_5 and eight carbonyl ligands. A crystallographic characterization of 2 revealed a central $Mo_2Co_3(\mu_5\text{-}N)$ core whose idealized C_{2v} geometry consists of a square-pyramidal Mo_2Co_3 architecture containing a pentametal-coordinated (five-electron-donating) nitrido ligand positioned slightly below the basal Mo_2Co_2 plane. Inclusion of the two Mo-coordinated C_5Me_5 ligands and ten carbonyl groups (three of which are doubly bridging) lowers the symmetry to the crystallographically imposed molecular mirror plane which passes through the apical Co and two basal Co atoms, the nitride atom, and one bridging and three terminal carbonyl groups. This 74-electron square-pyramidal metal cluster is electronically equivalent and structurally analogous to the prototype carbido cluster, $Fe_5(CO)_{15}(\mu_5\text{-}C)$, and the corresponding nitrido cluster, $Fe_5(CO)_{14}(\mu_2\text{-}H)(\mu_5\text{-}N)$. $(\eta^5\text{-}C_5Me_5)_3Mo_3Co_2(CO)_8(\mu_3\text{-}NH)(\mu_4\text{-}N)$ (1): recrystallized from CH_2Cl_2/hexane with one dichloromethane molecule of crystallization (1·CH_2Cl_2); triclinic; $P\bar{1}$; a = 12.066 (1) Å, b = 13.683 (1) Å, c = 15.410 (1) Å, α = 85.781 (2)°, β = 80.245 (6)°, γ = 69.060 (6)°, V = 2342 Å^3 at T = 295 K; d_{obsd} = 1.62 g/cm^3 vs d_{calcd} = 1.64 g/cm^3 for Z = 2; least-squares refinement for one independent 1·CH_2Cl_2 converged at $R_1(F)$ = 5.43% and $R_2(F)$ = 8.23% for 4369 independent data ($I > 3\sigma(I)$) and 286 variables. $(\eta^5\text{-}C_5Me_5)_2Mo_2Co_3(CO)_{10}(\mu_5\text{-}N)$ (2): recrystallized from hexane with one C_6H_{14} molecule of crystallization (2·hex); orthorhombic; $Cmc2_1$; a = 14.770 (2) Å, b = 28.846 (10) Å, c = 9.357 (2) Å, V = 3987 Å^3 at T = 295 K; d_{calcd} = 1.61 g/cm^3 for Z = 4; least-squares refinement for the independent one-half molecule converged at $R_1(F)$ = 3.76% and $R_2(F)$ = 4.05% for 1875 independent data ($I > 3\sigma(I)$) and 167 parameters.

Introduction

The synthesis of organometallic clusters via the cycloaddition of coordinatively unsaturated organometallic carbonyl fragments to ethylene-like organometallic dimers has been shown to be a broadly applicable, rational approach for obtaining new trimetallic cluster compounds.[2] The utility of this synthetic pathway has prompted us to investigate similar additions to the inorganic acetylene analogue, $Mo_2(\eta^5\text{-}C_5Me_5)_2(CO)_4$ (3).[3] Recently, we have reported the initial results of several reactions of 3 with metal carbonyl fragments which have led to the isolation of new tri- and tetrametallic mixed-metal clusters.[4-7] Because of our interest in the preparation and examination of the physicochemical behavior of nitrosyl-capped metal clusters (only a few of which have been isolated and characterized[8]), we sought to further extend this synthetic approach to include the addition of organometallic nitrosyl fragments to 3.

An attractive feature of metal carbonyl–nitrosyl complexes is that they can be photolytically activated to more than one reactive species. For example, photolysis of the 18-electron $Co(CO)_3NO$ molecule (4) could lead to (1) a metal-to-ligand charge-transfer photoprocess[9-12] with

(1) Based, in part, on the Ph.D. Thesis of C.P. Gibson, University of Wisconsin—Madison, 1985. Present address: Department of Chemistry, West Virginia University, Morgantown, WV 26506.

0276-7333/88/2307-0543$01.50/0